

Characterization of some xenogeneic biomaterials for periodontal regeneration

A. SOANCĂ^a, I. PERHAIȚA^b, M. MICLĂUȘ^c, A. FLOREA^a, S.-A. PETRUȚIU^a, M. BĂCIUȚ^a, A. ROMAN^a

^a"Iuliu Hațieganu" University of Medicine and Pharmacy, Cluj-Napoca, Romania

^bInstitute for Research in Chemistry "Raluca Ripan", Babeș-Bolyai University, Cluj-Napoca, Romania

^cNational Institute for Research and Development of Isotopic and Molecular Technologies, Cluj-Napoca, Romania

The purpose of this study was the physicochemical characterization of four commercially available xenogeneic materials recommended for periodontal regeneration. The investigation was performed by X-ray diffraction, scanning electron microscopy, Fourier transform infrared spectroscopy (FTIR) and thermal analysis. The xenogeneic materials are mixtures of amorphous and crystalline phases based on hydroxyapatite (HAP), with variable degrees of crystallinity and crystallite dimensions. They contain different amounts of water, collagen, and mineral phase based on A- and B-type carbonated HAP, with various hydroxylation degrees. The xenogeneic biomaterials are different regarding both the appearance form (granules, spongy block, and bone paste) and ultrastructure (from trabecular architecture to reticulate structure). The biomaterials characteristics are expected to affect their *in vivo* performance and to influence the outcome of the periodontal treatment.

(Received April 29, 2015; accepted May 7, 2015)

Keywords: Xenograft, Infrared spectroscopy, Thermal analysis, X-ray diffraction, Scanning electron microscopy

1. Introduction

The goal of periodontal therapy is the achievement of complete anatomical and functional regeneration of the periodontium. Thereby, different approaches were developed in the last years like the use of bone grafting materials to compensate the bone loss due to periodontal disease [1,2]. The bone graft materials should present some particular characteristics such as osteoinduction, osteoconduction, biocompatibility, appropriate resorption time in relation to bone formation, volume stability, satisfactory mechanical properties, and no risk of disease transmission [3].

There are various types of bone grafts, that include autografts (from one site to another in the same individual), allografts (from individuals of the same species but different genetic composition), xenografts (from other species) and alloplastic materials (synthetic) [2]. Xenogeneic biomaterials, usually of bovine and porcine origins, are the most popular bone grafting materials used in dentistry due to their similarity to human bone tissue [4,5]. The source bone is processed by different methods to eliminate the immunogenic components from the donor (cells/cells remnants) that could induce pro-inflammatory responses against the material [6,7].

The choice of the right type of xenograft biomaterial depends on the size and location of the bone tissue defect as well as on the structural, biological, and biomechanical properties of the graft itself [8]. The biological performances of the bone grafts is influenced by the composition of the material, the porosity and surface

roughness, the size of the particles, the crystallinity, the volume of the graft or the pH of the surrounding environment [9,10].

Many commercially available xenograft products with different composition, physicochemical properties and indications have been developed through the various processing methods. These materials have different appearance forms such as granules, block grafts, or more recently bone paste that influences the clinical outcome of the materials [11].

There is a lack of information regarding indications, effectiveness, processing technique and the content of organic and inorganic components of the commercially available xenogeneic materials [10, 12]. Many times, the practitioner is the one who chooses one grafting material over the other according to the commercial advertising or his personal preferences, and not necessarily based on scientific reasons [8, 13]. Several articles published data upon the physicochemical properties of synthetic and biological apatite, but there are few studies focused on commercial xenogeneic materials used for bone repair [5, 14-17].

The purpose of this study was to perform a specific characterization of some non investigated, commonly utilized xenogeneic biomaterials. Four of the most commercially available natural bone-based biomaterials on the Romanian market, used as grafting materials were taken into consideration. They were selected to encompass products with different tissue sources (bovine and porcine) and composition (single phase/mineral or double phase/mineral, and organic matrix). The selection included products from various manufacturers, obtained by

different processing techniques, covering a wide range of clinical applications. To the best of our knowledge, only one of the four xenogeneic materials was previously investigated in terms of the physicochemical properties, namely Bio-Oss (Geistlich Pharma AG) [5, 12, 15]. This one was included in our study as comparison term. The investigation was performed by means of Fourier transform infrared spectroscopy (FTIR), X-ray diffraction (XRD), thermogravimetric analysis (TGA) and simultaneous differential thermal analysis (SDTA), and scanning electron microscopy (SEM). The objective of the study was to underline the similarities and differences between the selected xenogeneic materials in order to

complete the information basis for the practitioner, facilitating the right material choice.

2. Experimental

2.1 Materials

Four commercially available xenogeneic materials, with different physical appearance forms, were investigated in this study. The main characteristics, as given by the manufacturers, are summarized in Table 1 [18-21]. The investigations were performed either on samples of the as-supplied materials, or on samples preliminary dried for 3 h at 100 °C, under nitrogen flow.

Table 1. General presentation of the investigated xenogeneic materials

Sample code	Product Name & Batch number	Manufacturer	Product Description
BO	Bio-Oss® Small granules (Lot:060615)	Geistlich Pharma AG/ CH-6110 Wolhusen Switzerland	* Mineral derived from cancellous bone of bovine origin; * Spongy granules of 0.25-1 mm
BOC	Bio-Oss Collagen® (Lot:070276)	Geistlich Pharma AG/ CH-6110 Wolhusen Switzerland	*Mineral derived from cancellous bone of bovine origin “suspended” in collagen (10 %) of porcine origin * Spongy rigid/dried block containing mineral granules of 0.25-1 mm (BioOss®)
NBB	Natural Bovine Bone® (Lot: 11BA42520)	aap Biomaterials GmbH /64807 Dieburg Germany	*Biomaterial derived from cancellous bone of bovine origin; *Protein free hydroxyapatite ceramic mineral similar to the human bone * Ceramic granules of 0.5-1mm;
OBP	OsteoBiol® Putty, (Lot:130260)	Tecnoss srl /10094 Giaveno (TO)- Italy	*Biomaterial derived from cortico-cancellous bone of porcine origin (specific code: HPT09S) *Bone mix (paste) with plastic consistency consisting of 80 % micronized bone mix (particle granulometry up to 300 µm); with additional 20 % collagen gel

2.2 Characterization of the xenogeneic materials

Scanning electron microscopy. The morphology, surface roughness and pores size of the bone substitutes were estimated using scanning electron microscopy (SEM) with a JEOL JSM-25S Scanning Microscope, at 30 kV. Samples were sputter-coated with gold, using an Automatic Sputter Coater (AGAR Scientific). The images were processed with a Deben Pixie-3000 image processor (Deben Ltd., Debenham, UK).

Infrared spectroscopy. Fourier transform infrared spectroscopy (FTIR) was conducted using solid phase analysis (KBr pellets technique). In this purpose, the preliminary dried biomaterials (100 °C, 3 h) as well as the thermally treated biomaterials (1,000 °C, 1 min) were mixed with potassium bromide (KBr for IR spectroscopy; Merck) and grounded mechanically in the agate mortar. The homogenized powder mixture (about 0.1 mg sample/30 mg KBr) was compressed using a manual die to produce a transparent pellet for FTIR spectroscopy. A Nicolet 6700 FTIR Spectrometer (ThermoScientific, USA) running the OMNIC™ software was used to collect the infrared spectra over the 400- 4,000 cm⁻¹ range. The spectra were baseline corrected, normalized, and analyzed

for both the inorganic and organic constituents of the biomaterials.

X-ray powder diffraction. X-ray powder diffraction (XRD) patterns were obtained with a Bruker D8 Advance diffractometer with CuK α radiation (40 kV, 30 mA), using alumina/corundum powder for instrument broadening correction. The measurements were performed on preliminary dried biomaterials, at room temperature, in the range $2\theta = 10-85^\circ$ (steps of 0.02°).

Thermal analysis. The thermal behaviour of the biomaterials was investigated with a Mettler Toledo thermal analysis instrument (TGA/SDTA851^e system, LF 1600°C) that allows the simultaneous measurement of mass and temperature changes indicating the chemical transformations and thermal events/ physical transitions during the sample heating. The investigation was performed on the as-supplied biomaterials, placed in platinum crucibles (150 µL), using amounts of about 20 mg each for BO, BOC and NBB samples or 40 mg for the very humid OBP material. The heating was carried out between room temperature and 1,200 °C, at a rate of 10 °C/min, in air flowing (50 mL/min).

3. Results and discussion

The present study is focused on the physicochemical characterisation of four commercially available xenogeneic bone substitute materials from various manufacturers, i.e.: Bio-Oss®, Bio-Oss Collagen® (Geistlich Pharma AG, Switzerland), Natural Bovine Bone® (aap Biomaterials GmbH, Germany) and OsteoBiol® Putty (Tecnos srl, Italy). The main characteristics, as indicated by the manufacturer are summarised in Table 1. Note that, for the simplicity, these commercial marks were encoded.

These xenogeneic materials are recommended for application in periodontology, implantology, oral surgery in different procedures, i.e. treatment of periodontal defects, peri-implant defects, extraction socket preservation, alveolar ridge preservation, sinus floor elevation, reconstruction of bone defects, etc. The selected xenografts have different appearance forms i.e. powders with various granule sizes (BO, NBB), spongy block (BOC) and extremely humid paste (OBP), that leads to different handling protocols. One can mention that BOC is in fact a derivative from BO biomaterial (see Table 1). The xenogeneic materials under discussion differ also with respect to the origin of the bone source that is bovine (BO, BOC, NBB) and porcine (OBP), and to their composition. Considering this, they are either single mineral phase (BO, NBB) or mineral-organic double phase biomaterials (BOC, OBP), due to the addition of porcine collagen. The latter allows a convenient handling and easier application of the xenogeneic material. Moreover, collagen is slowly resorbed and replaced by new bone cells/regenerative cells.

3.1 Scanning electron microscopy

The scanning electron microscopy analysis was used to investigate the morphological characteristics of the different bone grafts. Some representative SEM images of the xenogeneic materials, at different magnifications, are depicted in Figure 1.

The SEM images show different shapes and structural features for the materials. The two particulate materials, BO and NBB exhibit porous, irregular and sharp-edge particles with variable sizes. They present a rather rough surface and different size micropores, from 100-300 μm (NBB) to 200-1,000 μm (BO), as visible at 45 X and 300 X magnification. The higher magnification images (1500 X) illustrate that NBB powder consists in well defined, coalescent small grains, whereas BO biomaterial shows a mineral scaffold organization similar to the collagen fibres. It is obvious that, this material preserves the fibre-like structure of the collagen removed during the manufacturing processing, maintaining the original bone morphology [22].

The two double-phase materials, BOC and OBP have a reticulated appearance due to the collagen fibres. This aspect is most evident for the spongy block. The micrograph of the bone paste, which contains a large amount of water, reveals many cracks on the material surface formed during the SEM sample preparation (vacuum effect). The mineral granules of the two collagenated materials are hardly visible, due to their fibrous texture. In fact, the spongy block graft contains different size osseous particles packed together with collagen fibres, while the bone paste contains a mixture of small particles embedded in a collagen gel, ensuring an easier handling of the graft.

All investigated materials present a porous structure that could increase the surface area of the xenograft material, favouring cell adhesion, proliferation, and differentiation (osteoconduction) and bone growth [23, 24].

3.2 X-Ray diffraction

X-Ray powder diffraction was used to identify crystalline phase composition and to qualitatively evaluate the crystallinity of the materials. The X-ray diffraction patterns are shown in Figure 2. All detectable peaks could be indexed as belonging to the hexagonal hydroxyapatite $\text{Ca}_{10}(\text{PO}_4)_6(\text{OH})_2$ in the standard data (ICDD PDF2 card 74-0566).

The investigated xenogeneic materials are mixtures of crystalline and amorphous hydroxyapatite (HAP) and possess variable degree of structural order, as indicated by the different peak widths from the XRD patterns. The diffractograms of BO biomaterial exhibit broad peaks with a low signal-to-noise ratio, corresponding to low-crystallinity materials. On the other hand, the sharp and well-resolved XRD peaks of the NBB biomaterial indicate a highly crystalline hydroxyapatite. The diffractograms of BOC and OBP illustrate the dual-phase composition of these samples. In this case, the patterns present the characteristic XRD peaks of hydroxyapatite, superimposed on some broad band arising from amorphous collagen [5].

NBB, BO, BOC and OBP biomaterials differ by the amount of the crystalline phase and the size of the crystallites forming it. The degree of crystallinity was evaluated as being the ratio between the diffraction peaks area and the total area, which includes area of diffraction peaks and amorphous halos, using the MS Reflex Plus module within the Accelrys Materials Studio® suite [25]. The crystallite size of the crystalline phase was calculated from the full width at half maximum, FWHM, for (0 0 2) reflexion ($2\theta = 25.88^\circ$), by using the Scherrer formula $D = (K \times \lambda) / (\beta \times \cos\theta)$ where D is the apparent volume-weighted crystallite size, λ is the X-rays wavelength (1.54060 Å, in this case), K = 0.89 (the Scherrer constant), β is the width of line at the half-maximum intensity (in radians) and θ is the Bragg angle [26].

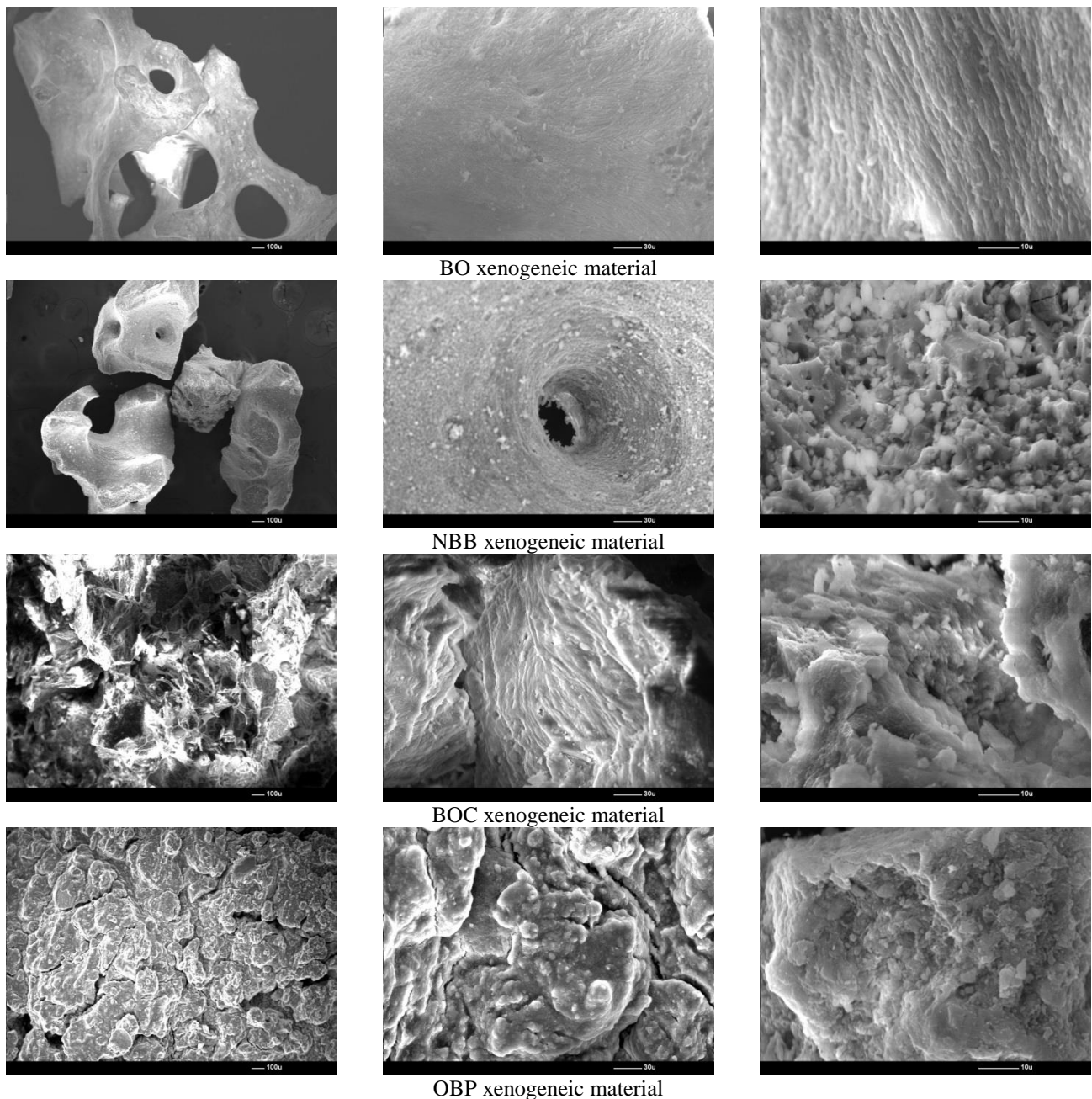


Fig. 1. Representative micrographs at different magnifications: 45 X (left), 300 X (middle) and 1500 X (right)

The degree of crystallinity and the average size of the crystallites in NBB, BO, BOC and OBP biomaterials are 61 %, 49 %, 50 % and 45 % and, correspondingly, 71 nm, 35 nm, 33 nm, and 30 nm. XRD results for BO biomaterial are in agreement with the literature data [15].

The diffraction lines of BO, BOC and OBP biomaterials are relative broad and weakly resolved, as compared with NBB biomaterial. The fact that NBB powder has a relative higher crystallinity degree and contains crystallites twice as large as the others suggests that this biomaterial was manufactured by a high temperature processing (already suggested by SEM images) [10, 27].

X-ray diffraction revealed that the only crystalline phase present in the selected biomaterials is calcium hydroxyapatite (HAP, $\text{Ca}_{10}(\text{PO}_4)_6(\text{OH})_2$). In fact, this hydroxyapatite-based composition of the natural bone-based biomaterials is the most important argument in their choice for grafting procedures. It is well known that, HAP shows excellent biocompatibility not only with hard tissue but also with soft tissue. This material is capable of integrating biologically when directly implanted into a bone defect; furthermore, it produces no harmful effect on the immune system, is not toxic, and features an osteoconductive behaviour [28,29].

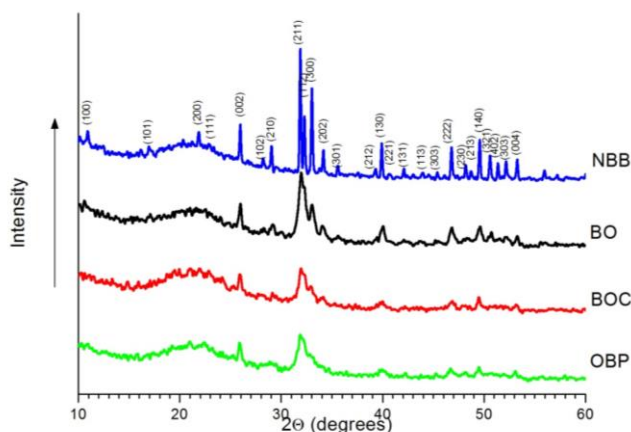


Fig. 2. XRD patterns of the investigated xenogenic materials (the peaks of the main reflexion planes are identified using 74-0566 PDF-card for hexagonal hydroxyapatite)

3.3 FTIR spectroscopy

FTIR spectroscopy provides information on all biomaterial components i.e. mineral phase and organic matrix. Figure 3 shows the absorption spectra of the dried biomaterials NBB, BO, BOC, OBP as well as the spectra of the thermally treated BO and BOC biomaterials (inset pictures). The major FTIR absorption frequencies in the 400-4,000 cm^{-1} spectral region, associated with the mineral phase are summarised in Table 2. The bands assignments are according to literature data [30-32].

The first group of vibrational spectra is related with collagen-free biomaterials. As expected, the infrared absorption spectra of BO and NBB samples show the typical bands originated from the hydroxyapatite mineral, i.e. the most intense PO_4 stretching and bending bands observed in the 900-1,200 cm^{-1} and, correspondingly, 500-600 cm^{-1} region [30]. BO biomaterial presents, in addition, some low-intensity vibration bands in the 1,380-1,580 cm^{-1} domain, that are characteristic to the carbonate substituted hydroxyapatite [15]. These bands disappear almost completely, when the biomaterial is thermally treated, due to the carbonate decomposition. Carbonate vibration bands are also missing in the FTIR spectrum of NBB biomaterial, thus suggesting that this one was manufactured by high temperature thermal treatment [15, 33].

The second group of vibrational spectra is dedicated to the collagenated BOC and OBP biomaterials. The characteristic vibration bands of both the organic matrix (collagen) and the mineral phase (carbonated hydroxyapatite) are noticed only in the infrared spectrum of OBP sample. The Amide I (C=O stretch), Amide II (N-H bend & C-N stretch) and Amide III (C-N stretch & N-H bend) bands could be identified in the 1,600-1,700 cm^{-1} , 1,500-1,600 cm^{-1} , and correspondingly 1,200-1,300 cm^{-1} domains, besides some CH_3 and CH_2 vibration bands (2,850-3,000 cm^{-1} range) [30,34]. In the case of BOC biomaterial, the specific collagen vibration bands are obscured by the strong mineral IR peaks, most probably

due to its relative small amount. Consequently, the spectra of BO and BOC biomaterials are very similar (apart from the 2,850-3,000 cm^{-1} region). According to the manufacturer (Table 1), BOC biomaterial contains only a small amount of collagen as to ensure the cohesion of the osseous particles and to reticulate the biomaterial in the block form, a xenogenic product more easily accommodated into defect.

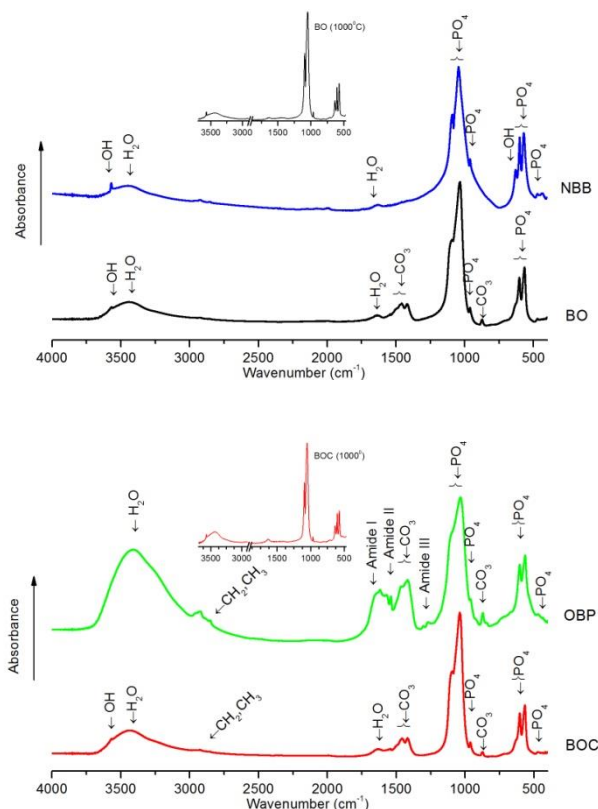


Fig. 3. FTIR spectra of the xenogenic materials: BO, NBB (up) and BOC, OBP (down). The spectra of the thermally treated BO and BOC sample are presented in the inset pictures.

The inset pictures illustrate that, during the thermal treatment in air, the carbonate phase and organic matrix are totally removed and the degree of the crystalline order increases (the phosphate bands become narrower). HAP crystalline structure is stable up to high temperatures [35].

FTIR patterns of almost all the investigated biomaterials contain also two vibration bands associated with the structural hydroxide ions from HAP, situated at about 3,570 and 630 cm^{-1} [22]. These two bands are well resolved especially in NBB biomaterial, reflecting both the HAP crystallinity and purity (no CO_3 impurity). Moreover, the sharpness of PO_4 bands indicates a rather well-crystallized hydroxyapatite [36]. Additionally, the biomaterials particles contain surface-adsorbed water (at least at the moment of IR data collection) and occluded H_2O , as revealed by the broad water band extending over

the range of 3,100-3,700 cm^{-1} and, correspondingly, the small band at about 1,640 cm^{-1} [37,38].

The IR absorbance signal positions and intensities may vary depending on the particular bond environment.

The position of the major FTIR frequencies of the mineral phase in the four investigated biomaterials is indicated in Table 2.

Table 2. Major FTIR absorption frequencies (in cm^{-1}) of the mineral phase of the investigated xenogenic materials and their assignments (br-broad band; sh-shoulder)

No	Xenogenic materials (cm^{-1})				Band assignment
	NBB	BO	BOC	OBP	Vibration type/ Significance
1.	3570	3570	3570	-	O-H Stretching (νOH)/Hydroxide ion
2.	3449(br)	3447(br)	3438 (br)	3407(br)	O-H Stretching ($\nu_1\text{H}_2\text{O}$)/Water molecules
3.	1635	1637	1637	~ 1638	H-O-H Bending ($\nu_2\text{H}_2\text{O}$)/Water molecules
4.		1541(sh)	1543(sh)	1540	C-O Stretching ($\nu_3\text{CO}_3$)/Carbonate ion
5.		1469(sh)	1467(sh)	1467(sh)	
6.		1458	1458	1452	
7.		1419	1418	1417	
8.	1091	1094	1094	1100(sh)	P-O Stretching ($\nu_3\text{PO}_4$)/Phosphate ion
9.	1044	1036	1038	1035	
10.	961	962	962	961	P-O Stretching ($\nu_1\text{PO}_4$)/Phosphate ion
11.	873 (sh)	874	874	872	O-C-O Bending ($\nu_2\text{CO}_3$)/Carbonate ion
12.	631	633 (sh)	633 (sh)	-	OH Libration($\nu_L\text{OH}$)/Hydroxide ion
13.	602	602	602	602	O-P-O Bending ($\nu_4\text{PO}_4$)/Phosphate ion
14.	570	570	570	570	
15.	473	469	472	469	O-P-O Bending ($\nu_2\text{PO}_4$)/Phosphate ion

The location of the phosphate vibration peaks is similar in all samples. The differences appear in relation with the IR bands associated with the other absorption groups. The small sharp O-H stretching band (3,570 cm^{-1}) is visible in NBB, BO and BOC biomaterials, whereas the OH libration band is well evidenced only in NBB sample (at 630 cm^{-1}), and appears as shoulder in BO or BOC biomaterials. It appears that, the investigated biomaterials possess variable degree of hydroxylation.

Only three of the investigated biomaterials contain significant amounts of structural carbonate. In calcium hydroxyapatite, $\text{Ca}_{10}(\text{PO}_4)_6(\text{OH})_2$, the carbonate ions could partially substitute both the phosphate and the hydroxyl ions of the HAP structure, giving rise to B- and A-type carbonated apatite, respectively. Depending on the substitution type, IR absorption bands may appear at slightly different wavenumbers. It is generally accepted that 1,546, 1,456, and 880 cm^{-1} are the characteristic bands of type A substitution and 1,465, 1,413, and 873 cm^{-1} of type B substitution [39]. FTIR spectroscopic data suggest that BO, BOC and OBP biomaterials contain both types of carbonate substituted hydroxyapatite. It can be noticed that, the resolution of both $\nu_3\text{PO}_4$ and νOH vibration bands diminished with increasing CO_3 [22]. Apparently, OH⁻ ion is totally substituted by carbonate in OBP biomaterial. However, the decrease of the hydroxylation degree of hydroxyapatite could be associated not only with the carbonate substitution, but also with the HAP crystalline ordering [40]. Whereas the highly crystalline NBB biomaterials has strong OH vibration bands (3,572 and 630 cm^{-1}), the poorly crystalline BO, BOC (and even OBP) materials have extremely weak bands at these positions.

The protein presence in both collagen-containing biomaterials, BOC and OBP is indirectly illustrated by the down-shift of the H_2O band, relative to NBB and BO biomaterials. This could be the effect of the two of the characteristic NH stretching vibrations associated with Amide A (about 3,300 cm^{-1}) and Amide B (about 3,100 cm^{-1}) of the peptide linkage [30, 34].

The vibrational spectra revealed that the investigated biomaterials consist from more or less crystalline hydroxyapatite, containing both A-type and B-type carbonate in the HAP lattice. This is in agreement with the literature data stipulating that the biological apatites consist usually from calcium-deficient carbonated hydroxyapatite [14, 42]. The presence of B-carbonate in the apatite lattice causes a decrease in crystallinity and an increase in solubility both *in vitro* and *in vivo* tests [43]. It was illustrated that the investigated biomaterials possess different hydroxylation degree. The low degree of hydroxylation of bone-based biomaterials might affect their functionality as xenograft [40]. It was also confirmed that water molecules are present in the crystal structure of non-stoichiometric apatite from natural bone biomaterials [44]. The FTIR spectroscopic data for BO biomaterial are in accordance with those from the literature [15, 22].

3.4 Thermal analysis

Thermogravimetric analysis and simultaneous differential thermal analysis TGA/SDTA were employed to complete the information about the investigated biomaterials. The thermogravimetric TG-curves of the four biomaterials (registered to monitor the mass changes with temperature/time) as well as DTA plots (registered to measure the temperature difference between the

biomaterial sample and the thermal system reference during the heating) and DTG plots of the collagenated biomaterials are depicted in Figure 4.

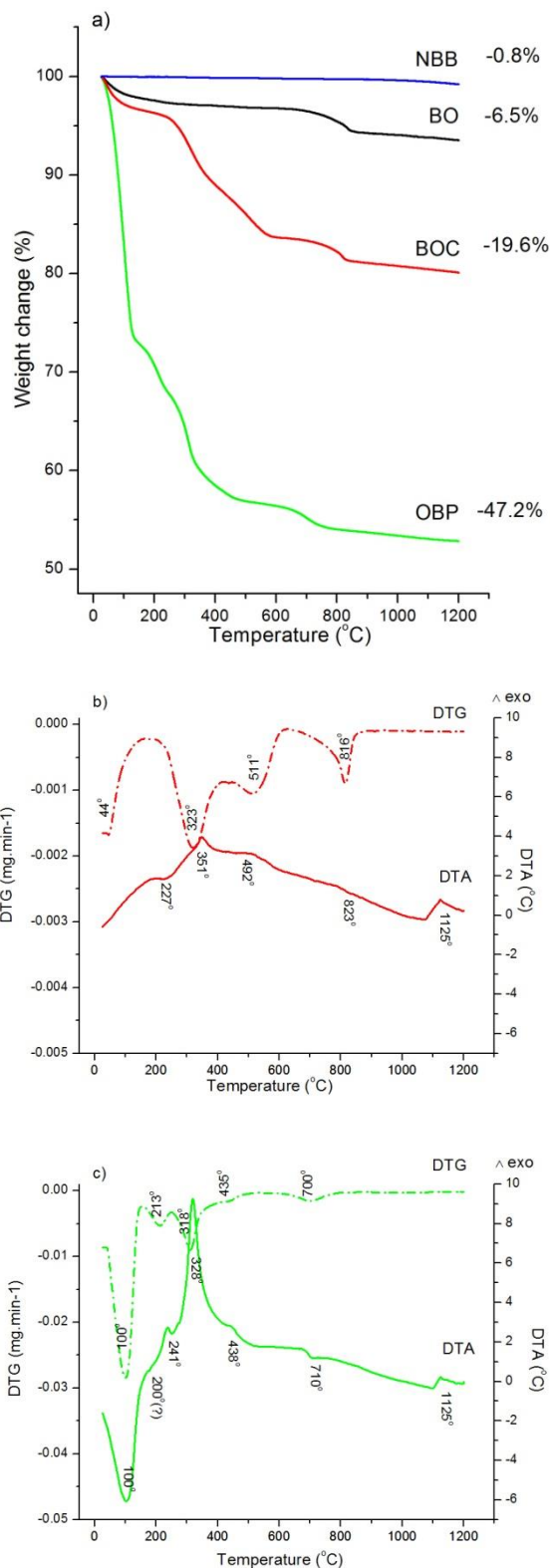


Fig. 4. Representative thermal analysis curves of the investigated xenogeneic materials, TGA plots (a) and DTG and DTA plots for the collagen-containing materials: BOC (b) and OBP (c)

The four materials have different thermal behaviour, when heated in air up to 1,200° C. The two single phase/mineral biomaterials exhibit the simplest TG pattern. NBB biomaterial shows a small, continuous weight loss (0.8 % of the initial weight) that could be correlated with water removal, either from internal pores or as consequence of the partial HAP dehydroxylation. BO biomaterial exhibits a total weight loss of 6.5 %, in two steps. The first step (25-200 °C) is associated with the drying process (removal of capillary pore residual water) whereas the last one (above 600 °C) is related to the partial dehydroxylation of HAP and the carbonate decomposition.

The two double phase/mineral phase and organic matrix biomaterials, BOC and OBP show apparently four and five weight loss steps, with a total mass decrease of 19.6 % and 47.2 %, respectively. The first (25-160 °C) and the last thermal stage (600-1,200 °C) are correlated with the removal of adsorbed water and correspondingly, to carbonate decomposition and HAP partial dehydroxylation. The intermediate two and three weight loss steps (between about 200 and 600 °C) are associated with the organics (collagen) removal [10].

Collagenated biomaterial BOC presents a total weight loss three times larger than the corresponding BO biomaterial (used for his manufacture) and about 2.5 times smaller than that of the OBP biomaterial.

TGA measurements were used to estimate the general chemical composition of the studied biomaterials (Table 3). The content of water and organic matrix in NBB, BO, BOC and OBP biomaterials was calculated based on the weight loss steps between 25-160 °C and 160-600 °C, whereas the amount of the apatite mineral was estimated by difference. The carbonate amount was determined on the basis of the weight loss between 600 and 900 °C (associated with the CO₂ release), and reported either to the initial biomaterial or to the material remaining after water removal (at 160 °C).

Table 3. Water, organic matrix, mineral phase, and carbonate content of the investigated xenogeneic materials, calculated from mass losses observed by TGA

Composition	Xenogeneic materials			
	NBB	BO	BOC	OBP
Water (wt %)	0.1	2.2	3.1	27.4
Organic matrix (wt %)	0	1.0	13.0	16.2
Mineral phase (wt %)	99.9	96.8	83.9	56.4
CO ₃ amount (wt %)*	0	3.4/3.5	3.6/3.7	3.7/5.1

* from the as-supplied xenogeneic materials / from the desiccated xenogeneic materials (160 °C weight value)

The highest level of water, organic matrix and apatite mineral was determined in OBP (27.4 wt %), OBP (16.2 wt %) and NBB (99.9 wt %), whereas the lowest level of them was found in NBB (0.1 wt %), BOC (13.0 wt %) and OBP (56.4 wt %), respectively. The values for the carbonate content are almost identical in BO, BOC and OBP biomaterials, when calculated from the as-supplied xenogeneic materials (3.4-3.7 wt % CO₃), but they are

quite different when they are given in relation to the desiccated xenogeneic materials. In the latter case, the carbonate amount becomes relative larger (5.1 wt %) for OBP biomaterial. NBB biomaterial does not contain organic matrix and carbonate impurity.

It should be mentioned that, the TGA calculated compositions are only estimative, for only the major weight loss steps were taken into consideration. Other processes such as removal of HAP lattice water (above 200 °C) or HAP dehydroxylation (above 400 °C) were ignored [45].

The weight loss stages as well as the thermal effects associated with them are well evidenced from the DTG and DTA plots depicted in Fig

4b and Figure 4c. The water and CO₂ removal takes place through endothermic processes, whereas the organics removal produces through exothermic ones. The exothermic maxima of the corresponding burning stages are at 351 and 492 °C, and 241, 328, and 438 °C for BOC and OBP biomaterials, respectively. For OBP biomaterial, the exothermic effects are relative stronger and develop at relative lower temperature, in comparison with BOC biomaterial, possibly due to the relative larger amount of water and collagen. The endothermic decomposition of the carbonate takes place at different temperatures. For BO, BOC, and OBP biomaterials, the rate of CO₂ release is maxim at 830 °C, 816°C, and correspondingly 700 °C, as indicated on the DTG curves. It is obvious that the protein burning accelerates the carbonate decomposition. NBB biomaterial does not contain carbonate, as already illustrated by FTIR spectra. It appears that, this product was manufactured at high temperature (above 800-900 °C).

It can be noted that, the DTA curves put in evidence one strong exothermic effect at about 1125 °C corresponding to a solid-solid transition (with no associated DTG peak). This could be explained if one takes into consideration that, the gradual, slow dehydroxylation of HAP leads to oxyhydroxyapatite/oxyapatite that transforms into β -tricalcium phosphate (β -TCP) and finally into α -TCP (with no weight change) [45].

These differences in chemical nature and phase composition, together with those detected in the sample morphostructural properties, are expected to affect the performance of these materials after their *in vivo* implantation.

4. Conclusions

The present study was focused on the physicochemical characterisation of four commercially available xenogeneic bone substitute materials from various manufacturers, i.e.: Bio-Oss® (BO), Bio-Oss Collagen® (BOC), Natural Bovine Bone® (NBB), and OsteoBiol® Putty (OBP). The similarities and differences between them were put in evidence by X-ray diffraction, scanning electron microscopy, FTIR spectroscopy and thermal analysis.

The investigated xenogeneic materials are based on hydroxyapatite, which is the only identified crystalline phase. They are amorphous-crystalline mixtures, with different degrees of crystallinity and crystallite dimensions. NBB has the highest crystallinity degree (61 %) and is formed from crystallites two times larger than BO, BOC and OBP biomaterial (about 70 nm in contrast to 30-35 nm). They contain A-type and B-type carbonate substituted HAP, excepting NBB that is CO₃-free. They also seem to possess different hydroxylation degree, excepting OBP that is hydroxyl-free.

The thermal behaviour of the materials is different, due mainly to their diverse composition; the collagenated biomaterials are similar in this respect, excepting the number of the apparent burning stages. The content of water, organic matrix and apatite mineral varies between 0.1 wt % (NBB) and 27.4 wt % (OBP), 0 wt % (NBB) and 16.2 wt % (OBP) and 99.9 % (NBB) and 27.7 wt % (OBP). The carbonate amount is comparable in BO and BOC (about 3.5 wt %), and relative larger relative to the OBP as-supplied product. It was confirmed that, NBB is protein- and carbonate-free, whereas OBP is a water- and protein-rich material.

The xenogeneic biomaterials are different regarding both their appearance form and ultrastructure. The single phase/mineral materials consist of granules with porous, bone-like “architecture” and rough surface. NBB is formed from slightly sintered well defined particles, whereas BO has a trabecular architecture, formed from much smaller grains. The dual-phase/mineral-organic matrix biomaterials show a reticulate structure. BOC biomaterial (the spongy block graft) contains different size osseous particles packed together with collagen fibres, whereas OBP (the bone paste) contains a mixture of small particles embedded in a collagen gel.

The physicochemical and morphostructural characteristics of the biomaterials are expected to affect their *in vivo* performance and to influence the outcome of the periodontal treatment. Being known that the carbonate and hydroxyl content could influence the biomaterial properties as substrate for cell growing, attention will be given to determine the HAP degree of carbonation and hydroxylation, in correlation with their crystallinity.

Acknowledgements

This paper was published under the frame of European Social Fund, Human Resources Development Operational Programme 2007-2013, project no. POSDRU/159/1.5/S/138776.

References

- [1] K.Hynes, D. Menicanin, S. Gronthos, P. Mark Bartold, *Periodontol* 2000, **59**, 203 (2012)
- [2] J Han, D Menicanin, S Gronthos, PM Bartold. *Aust Dent J*, **59** (Suppl 1), 117 (2014)
- [3] I Yip, Li Ma, N. Mattheos, M. Dard, N.P. Lang. *Clin Oral Implants Res*, **26**(5), 606 (2015)

- [4] S.Allegri Jr, B. Koenig Jr, M.R. Allegri, M. Yoshimoto, T. Gedrange, J. Fanghaenel, M. Lipski, *Ann Acad Med Stetin*, **54**, 70 (2008)
- [5] M.Figueiredo, J.Henriques, G.Martins, F.Guerra, F.Judas, H. Figueiredo, *J Biomed Mater Res Part B: Appl Biomater* **92B**, 409 (2010)
- [6] AA. Manfredi, A. Capobianco, ME. Bianchi, P. Rovere-Querini. *Crit Rev Immunol*, **29**(1), 69 (2009)
- [7] TJ Keane, R Londono, NJ Turner, SF Badylak. *Biomaterials*, **33**(6), 1771 (2012)
- [8] A. Figueiredo, P. Coimbra, A. Cabrita, F. Guerra, M. Figueiredo. *Mat Sci Eng C*, **33**, 3506 (2013)
- [9] C. Arcuri, F. Cecchetti, F. Germano, A. Motta, C. Santacroce, *Minerva Stomatol*, **54**, 351 (2005)
- [10] M.Figueiredo, A. Fernando, G. Martins, J. Freitas, F. Judas, H. Figueiredo, *Ceram Int*, **36**, 2383 (2010)
- [11] T. Karring, J. Lindhe. Concepts in tissue regeneration in Clinical periodontology and implant dentistry (Eds. J. Lindhe, N. P. Lang, T.Karring), Blackwell Munksgaard, Oxford, p.555 (2008).
- [12] S. Ghanaati, M Barbeck, P.Booms, J. Lorenz, CJ Kirkpatrick, RA Sader. *Acta Biomater*, **10**(8), 3557 (2014)
- [13] D.I.Ilan, *Oper Tech Plast Reconstr Surg*, **9**, 151 (2002).
- [14] J. Kolmas, M. Szwaja, W. Kolodziejski. *J Pharmaceut Biomed*, **61**, 136 (2012)
- [15] D.Tadic, M. Epple, *Biomaterials* **25**: 987 (2004)
- [16] G.A. da Cruz, S. de Toledo, E.A. Sallum, A.F.M. de Lima, *Braz Dent J*, **18**, 129 (2007)
- [17] T. Accorsi-Mendonça, M.B.Conz, TC Barros, L.Á. de Sena, G. de Almeida Soares, J. M. Granjeiro, *Braz Oral Res*, **22**(1), 5 (2008)
- [18] BioOss® Product information, <http://www.geistlich-pharma.com/en/dental/bone-substitutes/bio-oss/user-benefits/>
- [19] BioOss® Collagen Product Information, <http://www.geistlich-pharma.com/en/dental/bone-substitutes/bio-oss-collagen/user-benefits/>
- [20] Alpha-Bio's GRAFT Natural Bovine Bone, <http://www.alpha-bio.net/data/upl/brochures/>
- [21] Osteobiol® Putty. Product information, <http://www.tecnoss.com/putty.html>
- [22] F. de Paula do Desterro, M.Soaes Sader, G.D. de Almeida Soares, G.M. Vidigal Jr. *Braz Dent J*, **25**(4), 282 (2014)
- [23] J.Werner, B. Linner-Krcmar, W. Friess, P. Greil. *Biomaterials*, **23**(21), 4285 (2002)
- [24] A. Cruz, M. Pochapski, J. Daher, J. Silva, G. Pilatti, F.Santos. *J Oral Sci* **48**, 219 (2006)
- [25] Accelrys Software Inc. Materials Studio, Release 5.5. San Diego: Accelrys Software Inc (2010), <http://accelrys.com/products/materials-studio/index.html>
- [26] H.P. Klug, L.E. Alexander, *X-Ray Diffraction Procedures*, 2nd Ed., John Wiley & Sons Inc., p. 687 (1974)
- [27] K.D. Rogers, P. Daniels. *Biomaterials* **23**, 2577 (2002)
- [28] FV. Anghelina, DN. Ungureanu, V. Bratu, IN. Popescu, CO. Rusanescu. *Appl Surf Sci*, **285A**, 65 (2013)
- [29] V.S. Komlev, S.M. Barinov, V.P. Orlovskii, S.G. Kurdyumov, *Refract Ind Ceram*, **42**, 195 (2001)
- [30] M.M. Figueiredo, J.A.F. Gamelas, A.G. Martins. Characterization of Bone and Bone-Based Graft Materials Using FTIR Spectroscopy, in *Infrared Spectroscopy - Life and Biomedical Sciences* (Ed. Theophile Theophanides), InTech, Europe, Croatia, p 315 (2012)
- [31] L. Berzina-Cimdina, N. Borodajenko, Research of Calcium Phosphates Using Fourier Transform Infrared Spectroscopy, *Infrared Spectroscopy – Materials Science, Engineering and Technology*" (Ed. Theophile Theophanides), InTech, Europe, Croatia, p.123 (2012)
- [32] A. Antonakos, E. Liarokapis, T. Leventouri. *Biomaterials*, **28** (19), 3043 (2007)
- [33] A. Slosarczyk, Z. Paszkiewicz, C.Paluszkiwicz. *J Mol Struct*, **744–747**, 657 (2005)
- [34] A. Ficai, M.G.Albu, M. Birsan, M.Sonmez, D. Ficai, V. Trandafir, E. Andronescu. *J Mol Struct*, **1037**, 154 (2013)
- [35] S. Raynaud, E. Champion, D. Bernache-Assolant, P. Thomas. *Biomaterials*, **23**(4), 1065 (2002)
- [36] M.E. Fleet, X. Liu, P.L. King. *Am Mineral*, **89**, 1422 (2004)
- [37] DM. Ibrahim, AA Mostafa, SI Korowash. *Chem Cent J*, **5**, 74 (2011)
- [38] S.Yu. Venyaminov, F.G. Prendergast. *Anal Biochem*, **248**, 234 (1997)
- [39] F.Ren, Y. Ding, Y.Leng. *J Biomed Mater Res Part A*, **102A**, 496 (2014)
- [40] J.D. Pasteris, B.Wopenka, J.J. Freeman, K.Rogers, E. Valsami-Jones, J.A.M. van der Houwen, M.J. Silva., *Biomaterials*, **25**, 229 (2004)
- [41] J. Kong, S.Yu. *Acta Bioch Bioph Sin*, **39**(8), 549 (2007)
- [42] E. P. Paschalis. *Osteoporos Int*, **20**, 1043 (2009)
- [43] K. Rajendran, C. Dale Keefe. *Cryst Res Technol*, **45** (9), 939 (2010)
- [44] L. Yubao, CPAT. Klein, J. De Wijn, S. Van De Meer, K. De Groot. *J Mater Sci-Mater M*, **5**(5), 263 (1993)
- [45] K.Tonsuaadu, K.A. Gross, L. Pluduma, M.Veiderma. *J Therm Anal Calorim*, **110**: 647(2012)